대한영상의학회지

Texture Analysis of Gray-Scale Ultrasound Images for Staging of Hepatic Fibrosis
간 섬유화 단계 평가를 위한 회색조 초음파 영상 기반 텍스처 분석

Eun Joo Park, MD[1] , Seung Ho Kim, MD[1]* ,
Sang Joon Park, PhD[2] , Tae Wook Baek, MD[1]

[1]Department of Radiology, Inje University College of Medicine, Haeundae Paik Hospital, Busan, Korea
[2]Department of Radiology, Seoul National University Hospital, Seoul, Korea

*Corresponding author
Seung Ho Kim, MD
Department of Radiology,
Inje University,
College of Medicine,
Haeundae Paik Hospital,
875 Haeun-daero, Haeundae-gu,
Busan 48108, Korea.

Tel 82-51-797-0382
Fax 82-51-797-0379
E-mail radiresi@gmail.com

ORCID iDs
Eun Joo Park
https://orcid.org/0000-0003-2450-9365
Seung Ho Kim
https://orcid.org/0000-0002-9402-9642
Sang Joon Park
https://orcid.org/0000-0003-1013-681X
Tae Wook Baek
https://orcid.org/0000-0001-8743-022X

Purpose To evaluate the feasibility of texture analysis of gray-scale ultrasound (US) images for staging of hepatic fibrosis.

Materials and Methods Altogether, 167 patients who had undergone routine US and laboratory tests for a fibrosis-4 (FIB-4) index were included. Texture parameters were measured using a dedicated in-house software. Regions of interest were placed in five different segments (3, 5, 6, 7, 8) for each patient. The FIB-4 index was used as the reference standard for hepatic fibrosis grade. Comparisons of the texture parameters between different fibrosis groups were performed with the Student's t-test or Mann-Whitney U-test. Diagnostic performance was evaluated by receiver operating curve analysis.

Results The study population comprised of patients with no fibrosis (FIB-4 < 1.45, $n = 50$), mild fibrosis (1.45 ≤ FIB-4 ≤ 2.35, $n = 37$), moderate fibrosis (2.35 < FIB-4 ≤ 3.25, $n = 27$), and severe fibrosis (FIB-4 > 3.25, $n = 53$). Skewness in hepatic segment 5 showed a difference between patients with no fibrosis and mild fibrosis (0.2392 ± 0.3361, 0.4134 ± 0.3004, respectively, $p = 0.0109$). The area under the curve of skewness for discriminating patients with no fibrosis from those with mild fibrosis was 0.660 (95% confidence interval, 0.551–0.758), with an estimated accuracy, sensitivity, specificity of 64%, 87%, 48%, respectively.

Conclusion A significant difference was observed regarding skewness in segment 5 between patients with no fibrosis and patients with mild fibrosis.

Index terms Liver; Fibrosis; Ultrasound; Liver Disease; Computer; Software; Diagnosis

INTRODUCTION

Hepatitis B and C are the leading causes of chronic liver fibrosis in East Asia (1-4). Chronic liver fibrosis has the potential to develop into liver cirrhosis, which is a leading

risk factor of hepatocellular carcinoma (HCC) (1, 4, 5). Several studies have demonstrated that early antiviral treatment of viral hepatitis at the incipient stage is highly effective in improving and reversing hepatic fibrosis and liver cirrhosis (6, 7). Therefore, detection and staging of early liver fibrosis is crucial to the success of early treatment and prognosis.

The gold standard for staging of liver fibrosis is histopathologic diagnosis by biopsy (8). However, biopsy is problematic, due to its invasiveness and post procedural complications (9). Gray-scale ultrasound (US), by contrast, is superior for its high accessibility and non-invasiveness. However, the operator dependency of the examination remains a major demerit of diagnosing and staging of liver fibrosis by US. Moreover, US-based evaluation of liver parenchymal echogenicity is frequently discordant between operators, not only between expert and novice practitioners, but sometimes even between experts. In this regard, inter-observer variability can be a problem (10-12). Overall, US examination for detection and staging of liver fibrosis has the intrinsic limitation of being based on subjective assessment.

Fibroscan or US elastography represent quantitative methods for evaluation of liver fibrosis (13-19). However, these examinations incur additional expense by requiring specific devices or software programs. On the other hand, gray-scale US is readily available and less expensive.

Texture analysis is an emerging image analysis technique that has been showing promising results as a potential imaging biomarker based on CT and MR images (20-24). Texture analysis based on US images, though, has been relatively rarely studied. Quantitative studies on liver fibrosis grading by means of texture analysis, furthermore, are few (25, 26).

The purpose of the present study, therefore, was to investigate the feasibility of texture parameters of gray-scale US images for classification of liver fibrosis.

MATERIAL AND METHODS

This study was approved by the Institutional Review Board, which waived informed consent from patients (IRB No. 2018-12-013-001).

PATIENTS AND SELECTION CRITERIA

We searched the picture archiving and communication system (PACS) database records between November 2017 and September 2018 for patients with a history of viral hepatitis or chronic liver disease. Among 1962 patients, 437 satisfying the following inclusion criteria were initially enrolled: 1) underwent gray-scale US; 2) underwent laboratory blood tests including aspartate aminotransferase (AST), alanine aminotransferase (ALT), and platelet counts that were needed for calculation of the fibrosis-4 (FIB-4) index, which served as the reference standard for liver fibrosis grading (27-30). Among those 437 patients, 270 were excluded based on the following criteria: 1) underlying malignancy ($n = 3$); 2) underwent hepatectomy or segmentectomy ($n = 29$); 3) long time interval (> 30 days) between US and laboratory blood tests ($n = 185$); 4) US images of poor quality or that did not include all hepatic segments ($n = 53$). Therefore, 167 patients (66 men, 101 women; mean age, 59 years; range, 20–86) finally were included in the study.

Fig. 1. Screen capture of the workspace for measurements of texture parameters for the selected regions of interest shaded in green.
Automatically calculated texture parameters are displayed in the right column.
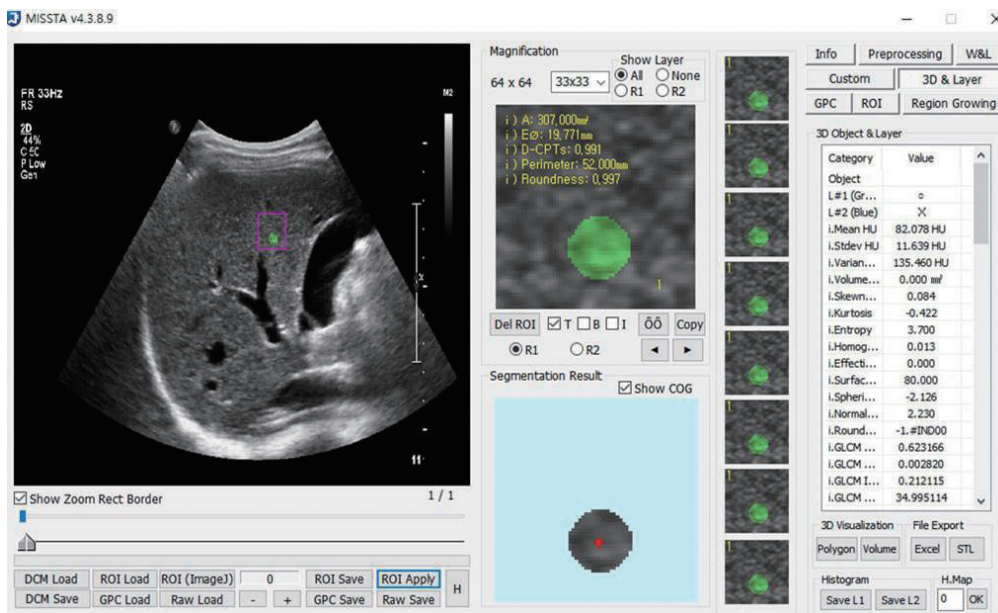
US EXAMINATION

US examinations were performed by three abdominal radiologist with 25, 20 and 14 years of clinical experience of abdominal US, respectively. The examination was done in conventional gray-scale US with a fundamental mode using the iU22 scanner (Philips Ultrasound, Bothell, WA, USA). C5-1 convex probes were utilized with a frequency setting of 4.0 MHz. The standard US protocol calls for imaging of both hemilivers. The left hemiliver images were obtained through the substernal and subcostal windows; the right hemiliver images were obtained through the subcostal and intercostal windows.

US TEXTURE ANALYSIS

The texture analysis was performed by one radiologist with three years of experience using an in-house software [Medical Imaging Solution for Segmentation and Texture Analysis (MISSTA), Seoul, Korea] with fully automated quantification of the texture features by dedicated C++ languages (Microsoft Foundation Classes; Microsoft, Redmond, WA, USA) (20-22). A circular region of interest (ROI) was placed in each of the five hepatic segments (three, five, six, seven and eight), taking care to avoid large vessels, focal hepatic lesions, and artifacts. To maintain consistency, the ROI contained 20 pixels (26). After placement of the ROI in each hepatic segment, the texture features were automatically calculated. The measurement was repeated in order to obtain intra-observer agreement. To evaluate inter-observer agreement, another radiologist with three years of experience performed the task with the same manner. Both radiologists were blinded to the results of each other. Fig. 1 shows the dedicated software workspace with the selected ROIs and calculated parameters. The texture parameters included first-order features based on gray-level histogram and second-order parameters based on gray-level co-occurrence matrix (GLCM). The first-order features consisted of the

following statistics: mean, standard deviation (SD), skewness, kurtosis, entropy and homogeneity. The second-order features included moment, angular second moment (ASM), inverse difference moment (IDM), contrast, and entropy (31).

REFERENCE STANDARD

The FIB-4 index was used as the reference standard because it can be non-invasively obtained and has been validated as having a good correlation to METAVIR score, not only in patients with hepatitis C, but also in those with hepatitis B or alcoholic liver disease (27-30, 32, 33). The FIB-4 index formula was as follows: age (years) $\times$ AST (U/L)/ [platelets (10^9/L) $\times$ ALT (U/L)]$^{1/2}$. The FIB-4 index's score of < 1.45 had a negative predictive value (NPV) for exclusion of fibrosis of 92% ($\leq$ METAVIR F2), and a score of > 3.25 had a positive predictive value (PPV) for confirmation of fibrosis of 76% ($\geq$ METAVIR F3) (27).

The METAVIR score conventionally represents the hepatic fibrosis grade. It consists of the degree of histological inflammatory activity (A0 = no activity, A1 = mild activity, A2 = moderate activity, A3 = severe activity) and the extent of fibrosis (F0 = no fibrosis, F1 = portal fibrosis without septa, F2 = portal fibrosis with few septa, F3 = numerous septa without cirrhosis, F4 = cirrhosis) (34). As earlier noted though, it requires an invasive liver biopsy, which incurs the risk of bleeding and sampling error. Nonetheless, it is still considered to be the hallmark of liver fibrosis on a histopathological basis.

STATISTICAL ANALYSIS

The texture parameters were compared between any two of the four fibrosis groups using the *t*-test or Mann-Whitney U test. When statistically significant parameters were found, accuracy, sensitivity, specificity, PPV and NPV were estimated by a receiver operating characteristic curve (ROC) analysis. The area under the ROC curve (AUC) was considered as the main indicator of diagnostic performance. Intra- and inter-observer agreements were calculated by the intraclass correlation coefficients (ICCs). The values were classified as poor (0.00–0.20), fair (0.21–0.40), moderate (0.41–0.60), good (0.61–0.80), and excellent (0.81–1.00). MedCalc software for Windows (MedCalc Software version 19.1.7, Mariakerke, Belgium) was used. A *p* value less than 0.0125 was considered a statistically significant difference after Bonferroni's correction for multiple comparisons.

RESULTS

The study population consisted of groups with no fibrosis (METAVIR F0, FIB-4 < 1.45, *n* = 50), mild fibrosis (F1, 1.45 $\leq$ FIB-4 $\leq$ 2.35, *n* = 37), moderate fibrosis (F2, 2.35 < FIB-4 $\leq$ 3.25, *n* = 27), and severe fibrosis (F3 + F4, FIB-4 > 3.25, *n* = 53) (Fig. 2). The demographics on the study population are summarized in Table 1.

Among the texture parameters, skewness in hepatic segment 5 showed statistically significant differences between no fibrosis and mild fibrosis (F0, 0.2392 $\pm$ 0.3361; F1, 0.4134 $\pm$ 0.3004, *p* = 0.0109) as well as moderate fibrosis (0.4292 $\pm$ 0.4542, *p* = 0.0104). Both kurtosis (F0, -0.2126 $\pm$ 0.5625; F3 + F4, 0.2686 $\pm$ 1.0251, *p* = 0.0042) and skewness (F0, 0.2362 $\pm$ 0.3361; F3 + F4, 0.4670 $\pm$ 0.4707, *p* = 0.0053) showed significant differences between no fibro-

Fig. 2. Gray-scale ultrasound images for each fibrosis group.
A-D. F0 (no fibrosis), FIB-4 index < 1.0 (A), F1 (mild fibrosis), 1 ≤ FIB-4 index < 1.45 (B), F2 (moderate fibrosis), 1.45 ≤ FIB-4 index ≤ 3.25 (C), and F3 + F4 (severe fibrosis), FIB-4 index > 3.25 (D).
FIB-4 = fibrosis 4
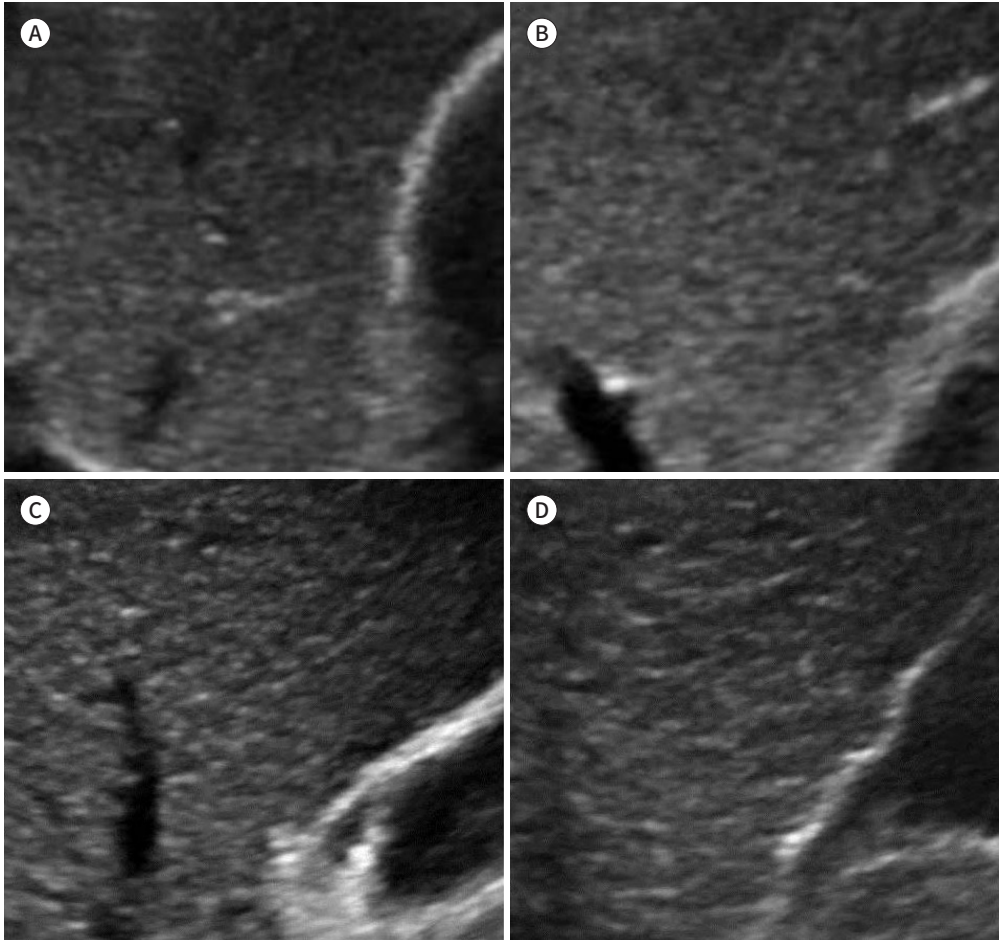
sis and severe fibrosis. In addition, SD showed a significant difference between mild fibrosis and severe fibrosis in segment 5 (F1, 8.2162 ± 2.1562; F3 + F4, 9.6086 ± 2.9597, p = 0.0110). The detailed results are summarized in Table 2. The other texture parameters, on the other hand, showed no significant differences in any of the five segments (p > 0.0125).

The AUC of skewness in segment 5 between no fibrosis and mild fibrosis was 0.660 (95% CI, 0.551–0.758); that of no fibrosis and moderate fibrosis was 0.616 (95% CI, 0.498–0.725). The estimated accuracy, sensitivity, specificity, PPV and NPV of skewness between no fibrosis and mild fibrosis were 64%, 87%, 48%, 55% and 83%, respectively; those of no fibrosis and moderate fibrosis were 57%, 74%, 48%, 43% and 77%, respectively. The AUCs between skewness and kurtosis discriminating no fibrosis and severe fibrosis showed no significant differences (p = 0.9663). The AUC of SD between mild fibrosis and severe fibrosis was 0.634 [95% confidence interval (CI), 0.527–0.733]. The detailed diagnostic predictive values are summarized in Table 3.

In terms of intra-observer agreement, ICCs for skewness, mean, SD, kurtosis, entropy and homogeneity, respectively were 0.83 (95% CI, 0.76–0.87), 0.93 (95% CI, 0.90–0.95), 0.66 (95%

Table 1. Demographic Data According to Fibrosis Grade

| Parameters | Fibrosis Grades | | | | |
	No Fibrosis (F0, $n = 50$)	Mild Fibrosis (F1, $n = 37$)	Moderate Fibrosis (F2, $n = 27$)	Severe Fibrosis (F3 + F4, $n = 53$)	Total ($n = 167$)
Age (years)	48.98 ± 13.77	58.14 ± 10.10	66.63 ± 11.09	65.04 ± 11.59	58.94 ± 13.78
Sex distribution (M:F)	18:32	14:23	9:18	25:28	66:101
AST (U/L)	23.72 ± 11.39	29.14 ± 12.46	29.85 ± 8.36	45.68 ± 24.42	32.88 ± 18.76
ALT (U/L)	26.22 ± 21.70	28.03 ± 17.99	25.15 ± 11.64	36.11 ± 33.15	29.59 ± 24.40
Platelet count	251.36 ± 68.94	172.62 ± 46.36	147.41 ± 43.45	95.87 ± 39.52	167.76 ± 80.51
FIB-4 index	0.99 ± 0.32	1.91 ± 0.26	2.79 ± 0.32	5.99 ± 2.75	3.06 ± 2.61
HCV positive	3	11	7	13	33
HBV positive	16	18	16	13	64
Alcoholic	0	1	0	12	13
Unknown	31	7	4	15	57

ALT = alanine aminotransferase, AST = aspartate aminotransferase, FIB-4 = fibrosis-4, HBV = hepatitis B virus, HCV = hepatitis C virus

CI, 0.54–0.75), 0.72 (95% CI, 0.62–0.79), 0.74 (95% CI, 0.65–0.81) and 0.87 (95% CI 0.83–0.91), respectively.

As for inter-observer agreement, ICCs for the above-mentioned features with the same order were 0.77 (95% CI, 0.68–0.83), 0.99 (0.95% CI, 0.98–0.99), 0.85 (95% CI, 0.79–0.89), 0.74 (95% CI, 0.65–0.81), 0.90 (95% CI, 0.87–0.93) and 0.97 (95% CI, 0.95–0.98), respectively. All features showed good or excellent agreements.

DISCUSSION

From the viewpoint of clinical implementation, it is very important to identify a mild fibrosis group that can be treated to reverse progression of hepatic fibrosis. Therefore, our finding that skewness showed an estimated accuracy of 64% in differentiating no fibrosis from mild fibrosis is noteworthy.

A previous study on hepatic fibrosis grade classification through quantification of US images showed promising results (25). Kvostikov et al. (25) reported that the diagnostic accuracy of a texture analysis of US images for classification of hepatic fibrosis grade was 73% using the best predictive classifier, namely k-nearest neighbors (KNN). Out of the training set, which consisted of F0 ($n = 7$), F1 ($n = 34$), F2 ($n = 8$), F3 ($n = 2$) and F4 ($n = 6$), they selected 22 parameters from 720 extracted ones and tested the data with machine-learning algorithms. The discrepancy in accuracy between the previous study and ours might be due to the usage of the best predictive algorithm, which can be considered to be a kind of radiomics approach. Therefore, we believe that additional and quantitative analyses of other parameters, such as liver edge or surface nodularity, have the potential to achieve improvement in the diagnosis and classification of liver fibrosis. However, the previous study's test set included only 7 cases (only one for each stage, except four cases for F1); thus, their observations should be verified in a larger cohort (25).

Computer-assisted imaging analyses currently are in the spotlight due to the increased at-

Table 2. Comparison of Texture Parameters Among Different Fibrosis Grades

Fibrosis Grades	Parameters										
	First-Order Statistics						Second-Order Statistics (GLCM-Based)				
	Mean (HU)	SD (HU)	Entropy	Homogeneity	Kurtosis	Skewness	ASM	Contrast	Entropy	IDM	Moments
No fibrosis (F0)	51.91 ± 18.03	8.46 ± 2.38	3.33 ± 0.28	0.025 ± 0.011	-0.21 ± 0.56	0.24 ± 0.34	0.0056 ± 0.0030	20.23 ± 9.50	2.46 ± 0.19	0.29 ± 0.066	0.27 ± 0.19
Mild fibrosis (F1)	45.14 ± 14.40	8.21 ± 2.16	3.30 ± 2.45	0.03 ± 0.01	0.02 ± 0.68	0.41 ± 0.30	0.0055 ± 0.0022	18.94 ± 8.90	2.44 ± 0.15	0.30 ± 0.052	0.20 ± 0.13
Moderate fibrosis (F2)	49.70 ± 16.86	8.88 ± 2.41	3.38 ± 0.24	0.026 ± 0.012	0.25 ± 1.32	0.43 ± 0.45	0.0052 ± 0.0024	21.38 ± 9.45	2.48 ± 0.16	0.29 ± 0.059	0.24 ± 0.18
Severe fibrosis (F3 + F4)	48.78 ± 17.70	9.61 ± 2.96	3.41 ± 0.28	0.027 ± 0.013	0.28 ± 1.04	0.46 ± 0.48	0.0054 ± 0.0025	21.73 ± 10.26	2.48 ± 0.17	0.29 ± 0.061	0.24 ± 0.19
p^{*}	0.0536	0.6236	0.6680	0.0842	0.0626	0.0109	0.4334	0.4688	0.6461	0.5342	0.0888
$p^{\dagger}$	0.5936	0.4636	0.4250	0.5643	0.0896	0.0104	0.7087	0.6144	0.5757	0.9886	0.6084
$p^{\ddagger}$	0.3757	0.0324	0.1773	0.3013	0.0037	0.0069	0.8023	0.4494	0.6110	0.9923	0.5137
$p^{\S}$	0.2600	0.2494	0.2361	0.3378	0.7696	0.6604	0.2991	0.2750	0.2207	0.5711	0.2930
$p^{\parallel}$	0.2836	0.0110	0.0455	0.5677	0.3106	0.4788	0.4738	0.1790	0.2432	0.4336	0.4163
$p^{\P}$	0.6289	0.2419	0.5152	0.6361	0.9506	0.4363	0.8364	0.7949	0.9069	0.9318	0.6728

*Comparison between no fibrosis group (F0) and mild fibrosis group (F1).
†Comparison between no fibrosis group (F0) and moderate fibrosis group (F2).
‡Comparison between no fibrosis group (F0) and severe fibrosis group (F3 + F4).
§Comparison between mild fibrosis group (F1) and moderate fibrosis group (F2).
‖Comparison between mild fibrosis group (F1) and severe fibrosis group (F3 + F4).
¶Comparison between moderate fibrosis group (F2) and severe fibrosis group (F3 + F4).
ASM = angular second moment, GLCM = gray-level co-occurrence matrix, HU = Hounsfield unit, IDM = inverse difference moment, SD = standard deviation

Table 3. Diagnostic Predictive Values of Statistically Significant Texture Parameters

Texture Parameters Comparisons	Skewness			Kurtosis	SD
	F0 and F1	F0 and F2	F0 and F3 + F4	F0 and F3 + F4	F1 and F3 + F4
Diagnostic Predictive Values					
AUC	0.660 (0.551–0.758)	0.616 (0.498–0.725)	0.662 (0.562–0.752)	0.664 (0.564–0.754)	0.634 (0.527–0.733)
Estimated accuracy (%)	64	57	64	66	58
Sensitivity (%)	87 (71.9–95.6)	74 (53.7–88.9)	78 (64.0–88.5)	56 (41.3–70.0)	30 (18.3–44.3)
Specificity (%)	48 (33.7–62.6)	48 (33.7–62.6)	51 (35.5–64.5)	76 (61.8–86.9)	94 (82.3–99.4)
PPV (%)	55	43	71	71	89
NPV (%)	83	77	60	61	49

Data in parenthesis are 95% confidence intervals.
AUC = area under the receiver operating characteristic curve, NPV = negative predictive value, PPV = positive predictive value, SD = standard deviation

tention paid to artificial intelligence (AI) in the area of radiology. AI including deep-learning systems creates algorithms based on self-learning and self-grouping of given information. There have been trials on the development and application of deep-learning systems for staging of liver fibrosis using CT images (35). Choi et al. (35) stated that their deep-learning system based on CT images for diagnosis of hepatic fibrosis had an accuracy of 79% and AUCs of 0.96, 0.97, and 0.95 for staging of significant fibrosis ($\geq$ F2, $\geq$ F3, and F4, respectively). Wu et al. (26), though they did not apply any deep-learning system, demonstrated that texture analysis in liver MR images can reflect fibrotic stages and necro-inflammatory activity grades. Their misclassification rates were 28%, 36%, and 20% for staging of fibrosis grade on T2-weighted, T1-weighted, and gadolinium-enhanced hepatocyte phase images, respectively. Lubner et al. (36) showed that texture parameters based on liver CT images could distinguish hepatic fibrosis grades; the AUCs for mean Hounsfield unit, skewness and kurtosis were 0.72, 0.86 and 0.87, respectively. Notably, skewness showed a sensitivity of 84% and a specificity of 75%.

In our study, the average SD of the severe fibrosis group was higher than that of the mild fibrosis group, in addition, the estimated maximum accuracy for differentiating between them was 58%. Similarly to our result, Lee et al. (37) observed that the average SD of chronic liver disease group (14.21 ± 2.32) was higher than those with normal liver group (11.0 ± 0.91) and suggested that SD could be used for distinguishing normal liver and chronic liver disease. However, they did not provide an optimal cut-off value or corresponding diagnostic predictive values to discriminate chronic liver disease from the control group.

As skewness and kurtosis increase, the difference between their pixel values increases, which reflects increased heterogeneity in the selected ROI (38). In our present study, as fibrosis progressed, increased skewness was observed, and in the severe fibrosis group relative to no fibrosis, increased kurtosis also was seen, which indicated increased heterogeneity of the liver parenchyma. Furthermore, higher SD reflected increased variation of intensity values, which in turn reflected increased heterogeneity of selected ROI.

Intriguingly, in contrast to the results from segment 5, the texture parameters obtained from the other hepatic segments (3, 6, 7 and 8) showed no statistical differences between the groups. This discrepancy could be explained by several factors. Gray-scale US of the liver is vulnerable to many artifacts dependent on scan depth, breathing or cardiac movement of

the patient, particularly in the left hemiliver. Not only in conventional US but also in liver elastography, liver fibrosis evaluation results are more reproducible and reliable in the right hemiliver than in the left (39). Therefore, we think that segment 5 is the optimal location for the US probe in texture analysis.

There are several limitations to our study. First of all, it was confined to an analysis of parenchymal echotexture. In conventional US, chronic liver disease is diagnosed based not only on parenchymal echotexture but also other features such as surface nodularity, liver volume, and liver edge. In fact, Choong et al. (40) reported that surface nodularity is the most sensitive sonographic feature for detection of significant hepatic fibrosis. Second, the FIB-4 index used as our reference standard did not reflect the exact histological fibrosis stage, as it can show only the range of calculated scores corresponding to the estimated grade of fibrosis. MR elastography might work as an alternative non-invasive global reference standard; however, problems involving additional cost and availability would be incurred. Therefore, the FIB-4 index was the second best option that we could choose as a non-invasive reference standard. In addition, it should also be emphasized that although we made an effort to correlate the FIB-4 index to the METAVIR score based on previous validation articles (27-30, 32, 33), the overlap of FIB-4 values between the different fibrosis groups (F0, F1, and F2) was inevitable because the cut-off values were arbitrarily chosen to maximize PPV or NPV. Therefore, misclassification bias might be incurred. Another issue might be raised in terms of adopting the same cut-off values of FIB-4 index to patients with Hepatitis B virus (HBV) and alcoholic liver disease. Though the cut-off values were established in patients with Hepatitis C virus (HCV), the overall diagnostic accuracy of FIB-4 index was not very high, but moderate in patients with HBV and alcoholic liver disease, which might negatively affect our results.

In conclusion, skewness showed a significant difference between the no fibrosis and mild fibrosis groups in segment 5.

Author Contributions

Conceptualization, K.S.H.; data curation, K.S.H., P.E.J.; formal analysis, K.S.H., P.E.J.; investigation, K.S.H., P.E.J.; methodology, K.S.H., P.E.J.; project administration, K.S.H.; resources, all authors; software, P.S.J.; supervision, K.S.H.; validation, all authors; visualization, P.E.J., K.S.H.; writing—original draft, all authors; and writing—review & editing, all authors.

Conflicts of Interest

The authors have no potential conflicts of interest to disclose.

Acknowledgments

REFERENCES

1. Schuppan D, Afdhal NH. Liver cirrhosis. *Lancet* 2008;371:838-851
2. Perz JF, Armstrong GL, Farrington LA, Hutin YJ, Bell BP. The contributions of hepatitis B virus and hepatitis C virus infections to cirrhosis and primary liver cancer worldwide. *J Hepatol* 2006;45:529-538
3. Bosch FX, Ribes J, Cléries R, Díaz M. Epidemiology of hepatocellular carcinoma. *Clin Liver Dis* 2005;9:191-211
4. Fattovich G, Stroffolini T, Zagni I, Donato F. Hepatocellular carcinoma in cirrhosis: incidence and risk fac-

대한영상의학회지

tors. *Gastroenterology* 2004;127:S35-S50

5. Ghany MG, Strader DB, Thomas DL, Seeff LB; American Association for the Study of Liver Diseases. Diagnosis, management, and treatment of hepatitis C: an update. *Hepatology* 2009;49:1335-1374

6. Serpaggi J, Carnot F, Nalpas B, Canioni D, Guéchot J, Lebray P, et al. Direct and indirect evidence for the reversibility of cirrhosis. *Hum Pathol* 2006;37:1519-1526

7. Dufour JF, DeLellis R, Kaplan MM. Regression of hepatic fibrosis in hepatitis C with long-term interferon treatment. *Dig Dis Sci* 1998;43:2573-2576

8. Manning DS, Afdhal NH. Diagnosis and quantitation of fibrosis. *Gastroenterology* 2008;134:1670-1681

9. Rockey DC, Caldwell SH, Goodman ZD, Nelson RC, Smith AD; American Association for the Study of Liver Diseases. Liver biopsy. *Hepatology* 2009;49:1017-1044

10. Strauss S, Gavish E, Gottlieb P, Katsnelson L. Interobserver and intraobserver variability in the sonographic assessment of fatty liver. *AJR Am J Roentgenol* 2007;189:W320-W323

11. Berzigotti A, Castera L. Update on ultrasound imaging of liver fibrosis. *J Hepatol* 2013;59:180-182

12. Tchelepi H, Ralls PW, Radin R, Grant E. Sonography of diffuse liver disease. *J Ultrasound Med* 2002;21:1023-1032

13. Ahn SJ, Lee JM, Chang W, Lee SM, Kang HJ, Yang H, et al. Prospective validation of intra- and interobserver reproducibility of a new point shear wave elastographic technique for assessing liver stiffness in patients with chronic liver disease. *Korean J Radiol* 2017;18:926-935

14. Ferraioli G, Parekh P, Levitov AB, Filice C. Shear wave elastography for evaluation of liver fibrosis. *J Ultrasound Med* 2014;33:197-203

15. Ferraioli G, Tinelli C, Zicchetti M, Above E, Poma G, Di Gregorio M, et al. Reproducibility of real-time shear wave elastography in the evaluation of liver elasticity. *Eur J Radiol* 2012;81:3102-3106

16. Shen QL, Chen YJ, Wang ZM, Zhang TC, Pang WB, Shu J, et al. Assessment of liver fibrosis by Fibroscan as compared to liver biopsy in biliary atresia. *World J Gastroenterol* 2015;21:6931-6936

17. Srinivasa Babu A, Wells ML, Teytelboym OM, Mackey JE, Miller FH, Yeh BM, et al. Elastography in chronic liver disease: modalities, techniques, limitations, and future directions. *Radiographics* 2016;36:1987-2006

18. Barr RG, Ferraioli G, Palmeri ML, Goodman ZD, Garcia-Tsao G, Rubin J, et al. Elastography assessment of liver fibrosis: society of radiologists in ultrasound consensus conference statement. *Radiology* 2015;276: 845-861

19. Jeong WK, Lim HK, Lee HK, Jo JM, Kim Y. Principles and clinical application of ultrasound elastography for diffuse liver disease. *Ultrasonography* 2014;33:149-160

20. Ahn SJ, Kim JH, Park SJ, Han JK. Prediction of the therapeutic response after FOLFOX and FOLFIRI treatment for patients with liver metastasis from colorectal cancer using computerized CT texture analysis. *Eur J Radiol* 2016;85:1867-1874

21. Choi TW, Kim JH, Park SJ, Ahn SJ, Joo I, Han JK. Risk stratification of gallbladder polyps larger than 10 mm using high-resolution ultrasonography and texture analysis. *Eur Radiol* 2018;28:196-205

22. Park HJ, Kim JH, Choi SY, Lee ES, Park SJ, Byun JY, et al. Prediction of therapeutic response of hepatocellular carcinoma to transcatheter arterial chemoembolization based on pretherapeutic dynamic CT and textural findings. *AJR Am J Roentgenol* 2017;209:W211-W220

23. Liu L, Liu Y, Xu L, Li Z, Lv H, Dong N, et al. Application of texture analysis based on apparent diffusion coefficient maps in discriminating different stages of rectal cancer. *J Magn Reson Imaging* 2017;45:1798-1808

24. Jalil O, Afaq A, Ganeshan B, Patel UB, Boone D, Endozo R, et al. Magnetic resonance based texture parameters as potential imaging biomarkers for predicting long-term survival in locally advanced rectal cancer treated by chemoradiotherapy. *Colorectal Dis* 2017;19:349-362

25. Kvostikov AV, Krylov AS, Kamalov UR. Ultrasound image texture analysis for liver fibrosis stage diagnostics. *Program Comput Soft* 2015;41:273-278

26. Wu Z, Matsui O, Kitao A, Kozaka K, Koda W, Kobayashi S, et al. Hepatitis C related chronic liver cirrhosis: feasibility of texture analysis of MR images for classification of fibrosis stage and necroinflammatory activity grade. *PLoS One* 2015;10:e0118297

27. Vallet-Pichard A, Mallet V, Nalpas B, Verkarre V, Nalpas A, Dhalluin-Venier V, et al. FIB-4: an inexpensive and accurate marker of fibrosis in HCV infection. comparison with liver biopsy and fibrotest. *Hepatology* 2007;46:32-36

28. Sterling RK, Lissen E, Clumeck N, Sola R, Correa MC, Montaner J, et al. Development of a simple noninva-

sive index to predict significant fibrosis in patients with HIV/HCV coinfection. *Hepatology* 2006;43:1317-1325

29. Sumida Y, Yoneda M, Hyogo H, Itoh Y, Ono M, Fujii H, et al. Validation of the FIB4 index in a Japanese nonalcoholic fatty liver disease population. *BMC Gastroenterol* 2012;12:2

30. Shah AG, Lydecker A, Murray K, Tetri BN, Contos MJ, Sanyal AJ; Nash Clinical Research Network. Comparison of noninvasive markers of fibrosis in patients with nonalcoholic fatty liver disease. *Clin Gastroenterol Hepatol* 2009;7:1104-1112

31. Castellano G, Bonilha L, Li LM, Cendes F. Texture analysis of medical images. *Clin Radiol* 2004;59:1061-1069

32. Yin Z, Zou J, Li Q, Chen L. Diagnostic value of FIB-4 for liver fibrosis in patients with hepatitis B: a meta-analysis of diagnostic test. *Oncotarget* 2017;8:22944-22953

33. Chrostek L, Przekop D, Gruszewska E, Gudowska-Sawczuk M, Cylwik B. Noninvasive indirect markers of liver fibrosis in alcoholics. *Biomed Res Int* 2019;2019:3646975

34. Bedossa P; French METAVIR Cooperative Study Group. Intraobserver and interobserver variations in liver biopsy interpretation in patients with chronic hepatitis C. *Hepatology* 1994;20:15-20

35. Choi KJ, Jang JK, Lee SS, Sung YS, Shim WH, Kim HS, et al. Development and validation of a deep learning system for staging liver fibrosis by using contrast agent-enhanced CT images in the liver. *Radiology* 2018;289:688-697

36. Lubner MG, Malecki K, Kloke J, Ganeshan B, Pickhardt PJ. Texture analysis of the liver at MDCT for assessing hepatic fibrosis. *Abdom Radiol (NY)* 2017;42:2069-2078

37. Lee CH, Choi JW, Kim KA, Seo TS, Lee JM, Park CM. Usefulness of standard deviation on the histogram of ultrasound as a quantitative value for hepatic parenchymal echo texture; preliminary study. *Ultrasound Med Biol* 2006;32:1817-1826

38. Materka A, Strzelecki M. *Texture analysis methods-a review. Technical university of lodz, institute of electronics, COST B11 report*. Brussels: Technical University of Lodz 1998

39. Jaffer OS, Lung PFC, Bosanac D, Patel VM, Ryan SM, Heneghan MA, et al. Acoustic radiation force impulse quantification: repeatability of measurements in selected liver segments and influence of age, body mass index and liver capsule-to-box distance. *Br J Radiol* 2012;85:e858-e863

40. Choong CC, Venkatesh SK, Siew EP. Accuracy of routine clinical ultrasound for staging of liver fibrosis. *J Clin Imaging Sci* 2012;2:58

간 섬유화 단계 평가를 위한 회색조 초음파 영상 기반 텍스처 분석

박언주[1] · 김승호[1*] · 박상준[2] · 백태욱[1]

목적 간 섬유화 단계 평가를 위한 회색조 초음파 영상 기반 텍스처 분석 측정 변수들의 진단적 유용성에 대해 평가한다.

대상과 방법 간 회색조 초음파 검사를 시행한 총 167명의 환자를 대상으로 하였다. 텍스처 분석은 한 명의 의사가 전용 소프트웨어를 이용하여 시행하였으며 3, 5, 6, 7, 8번 간 분절에 20 픽셀에 해당하는 원형 관심 영역을 지정하여 측정하였다. 간 섬유화 정도에 대한 표준 품으로는 fibrosis-4 (이하 FIB-4 index)를 사용하였다. 산출된 텍스처 변수들과 간의 섬유화 정도의 비교는 t-검정과 Mann-Whitney U 검정을 사용하였으며, 진단적으로 유의한 변수들에 대하여 수신자 운영 특성 곡선의 곡선 하 면적(area under the receiver operating characteristic curve)으로 진단능을 평가하였다.

결과 연구에 포함된 환자는 정상군(FIB-4 < 1.45, $n = 50$), 경도($1.45 \leq$ FIB-4 ≤ 2.35, $n = 37$), 중등도($2.35 <$ FIB-4 ≤ 3.25, $n = 27$)와 중증 간 섬유화군(FIB-4 > 3.25, $n = 53$)으로 구분되었다. 간의 5번 분절에서 왜도는 정상군과 경도군 사이에서 통계적으로 유의한 차이를 보였다(각각 0.2392 ± 0.3361, 0.4134 ± 0.3004, $p = 0.0109$). 정상군과 경도군을 구별하기 위한 왜도의 곡선 하 면적은 0.660 (95% confidence interval, 0.551–0.758) 이었으며, 추정 정확도, 민감도, 특이도는 각각 64%, 87%, 48%로 산출되었다.

결론 왜도는 5번 간 분절에서 정상군과 경도 섬유화군을 구분하는 데 유의한 차이를 보였다.

[1]인제대학교 의과대학 해운대백병원 영상의학과, [2]서울대학교병원 영상의학과